Magnetovolume instabilities and ferromagnetism versus antiferromagnetism in bulk fcc iron and manganese

V. L. Moruzzi and P. M. Marcus
IBM Thomas J. Watson Research Center, P.O. Box 218, Yorktown Heights, New York 10598

J. Kübler
Technical University of Darmstadt, D-6100 Darmstadt, West Germany
(Received 26 September 1988)

Total-energy band calculations, including an antiferromagnetic extension of the fixed-spin-moment procedure, are used to study magnetovolume effects in bulk fcc iron and maganese. By constraining these systems to have a fixed total magnetic moment in a single-atom fcc unit cell, we find magnetovolume instabilities in the form of first-order transitions from nonmagnetic to ferromagnetic behavior. Constraining the moments to have fixed values in a CuAu unit cell of two atoms to allow for antiferromagnetic (and field-induced ferrimagnetic) order alters these instabilities and yields second-order transitions from nonmagnetic to antiferromagnetic behavior at volumes coincident with the equilibrium volumes for both metals.

I. INTRODUCTION

Although iron, under normal conditions, has a ferromagnetic ground state and the bcc crystal structure, there has long been considerable interest in the fcc (γ) form which exists at high temperature and which can be stabilized by precipitation in a copper matrix.[1] This interest has been recently intensified by the successful stabilization of thin epitaxial layers of fcc iron on fcc copper[2,3] substrates, and by new work on Invar[4] alloys which contain iron in a fcc environment. Since experimental evidence for both antiferromagnetic and ferromagnetic order is found in these epitaxially stabilized structures, a study of the volume ranges of stability of the different forms of magnetic order is interesting. There is a similar interest in manganese which has complicated crystal structures but also exists in both the fcc and bcc form at high temperatures. The simpler forms of manganese are of current interest because they may be stabilized by epitaxial growth on cubic substrates.[5] In this case, the form of magnetic order (or lack thereof) is also of interest.

A number of band-theoretical treatments have demonstrated that fcc iron can be antiferromagnetic in certain volume ranges. Kübler[6] used a total-energy augmented-spherical-wave (ASW) method to show that this system can be nonmagnetic, ferromagnetic, or antiferromagnetic. Although fcc iron was initially found to have an antiferromagnetic ground state, subsequent work[7] showed the antiferromagnetic and nonmagnetic solutions to have almost identical total energies at equilibrium. Later work by Wang, Klein, and Krakauer,[8] based on a full-potential linearized augmented-plane-wave method, yielded similar results, and, in addition, found evidence for a low-spin ferromagnetic solution. Using a disordered-local-moment model, Pinski *et al.*[9] also find a transition from zero to finite local moments with antiferromagnetic interactions as volume is increased.

Using total-energy band calculations, Kübler also found evidence for antiferromagnetism in fcc[7] (and bcc[10]) manganese. More recently, Fry *et al.*[11] used Stoner theory and q-dependent susceptibility to predict an antiferromagnetic state for fcc manganese. Recent ASW results[12] based on a fixed-spin-moment (FSM) method[13] map the volume range of existence for the nonmagnetic, and the low-spin and high-spin ferromagnetic states for fcc iron. With increasing volume, the system was shown to undergo two successive first-order transitions, first from nonmagnetic to low-spin, and then to high-spin behavior, demonstrating that the system undergoes a series of magnetovolume instabilities. This latter result, which does not consider antiferromagnetic ordering, has also been obtained by Krasko[14] using a Stoner analysis, and has been used by Marcus and Moruzzi[15] to demonstrate that band-theory results are equivalent to a generalized Stoner[16] analysis in which the Stoner parameter is a function of magnetic moment and volume.

Band-theoretical evidence for magnetovolume instabilities in both bcc and fcc manganese is implicit in our earlier total-energy work[17] and in the results of Brener *et al.*[18] Neither of these studies considered antiferromagnetic order. The present work extends our earlier calculations of fcc iron to include both antiferromagnetic and ferrimagnetic order, and considers ferromagnetic, antiferromagnetic, and ferrimagnetic order for fcc manganese. In the present calculations, we remove the constraint that the systems can only have ferromagnetic order by considering a two-atom CuAu unit cell, thereby permitting one form of antiferromagnetic and ferrimagnetic order to develop. We use ASW spin-polarized band calculations[19] with the local density approximation and an extension of the FSM method to study magnetovolume effects in fcc iron and manganese over an extended volume range. Our results demonstrate that the removal of simplifying constraints used to facilitate band calculations can lead to the removal of magnetovolume instabili-

ties. That is, the constraints implicit in the model used in the calculations preselect particular solutions. With the removal of ferromagnetic constraint, we now find, in agreement with Kübler[6,7] and with Wang *et al.*,[8] that both systems have a tendency for antiferromagnetic rather than ferromagnetic order. In addition, we show that the onset of magnetic behavior coincides with the equilibrium volume and that antiferromagnetism is favored over a considerable range of volume expansion.

II. FSM ANTIFERROMAGNETISM

The FSM method is a procedure for doing total-energy spin-polarized band calculations at a given volume for a system constrained to have a fixed magnetic moment M. The basic calculated quantity is the total energy E, which varies with M. The moment may be considered to be constrained to have the fixed value by an effective externally applied magnetic field given by $H=dE/dM$. For the given volume, stable solutions are represented by M values corresponding to points where $H=dE/dM=0$ and $d^2E/dM^2>0$.

The idea of the FSM method, namely of imposing additional constraints on the band calculation to select particular types of solutions, can be readily extended to other magnetic states, including antiferromagnetic and ferrimagnetic states. In Fig. 1 we show total energy versus magnetic moment curves obtained with three different types of constraint for fcc iron at a volume V corresponding to a Wigner-Seitz radius, $r_{WS}=2.68$ a.u., where $V=(4\pi/3)r_{WS}^3$. The curve labeled nonmagnetic (NM), low spin (LS), and high spin (HS) corresponds to the constrained ferromagnetic case in which the moment of every atom in the system must have the same magnitude and direction. The NM, LS, and HS zero-field solutions, corresponding to the three local minima, imply a coexistence of three different solutions at this volume.

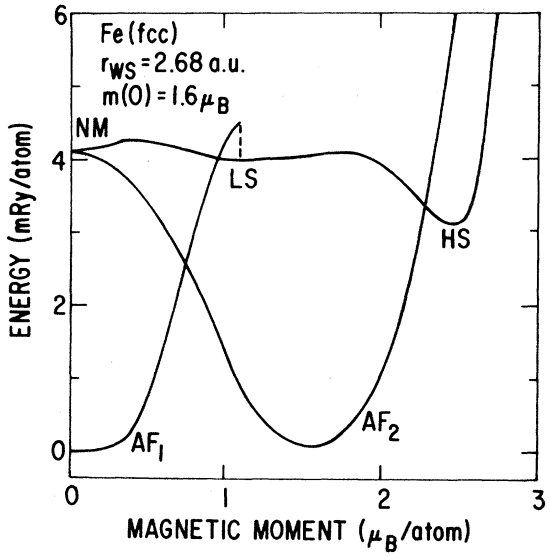

FIG. 1. Calculated total energies vs fixed moment for fcc iron for $r_{WS}=2.68$ a.u. The nonmagnetic, low-spin, and high-spin solutions are labeled on the curve corresponding to a ferromagnetic constraint. The curve labeled AF_1 corresponds to a FSM calculation in which two inequivalent iron atoms are arranged on a CuAu lattice to allow for antiferromagnetism. For these two cases, the total moment is constrained to have the indicated value. The curve labeled AF_2 also corresponds to a CuAu calculation, but here, the individual local moments are constrained to be equal and opposite. In this case, the total moment is zero and the local moments have the indicated values.

The curve labeled AF_1 corresponds to a two atom per unit cell calculation in the CuAu structure with the *total* moment constrained to have a given value and the two local moments free to adjust so as to minimize the total energy. This structure corresponds to type-I antiferromagnetism (AF) in which (001) planes have alternating local moments. Here, the algebraic sum of the individual local moments is required to be M. At $M=0$, the two local moments are equal and opposite, i.e., the solution at $M=0$ which minimizes the total energy yields local moments of plus and minus $1.6\mu_B$. The solutions at any finite total moment actually correspond to ferrimagnetic solutions in which the local moments are unequal, but sum to the constrained total moment. The curve labeled AF_2 corresponds to a different constraint on the two-atom cell. In this case, the two atoms are constrained to have *equal but opposite* local moments with zero total moment. That is, the local moments are not free to adjust, but have the prescribed values given in the figure.

The three calculations represented in Fig. 1 have a certain amount of overlap. First, note that at $M=0$ the AF_2 results coincide with the NM solution found with the ferromagnetic constraint. Since the local moments are zero for both constraints, this coincidence in the total energy is expected. Next, note that the minimum for the AF_2 curve occurs at the same energy as the minimum for the AF_1 curve. The energy coincidence of these two solutions implies identical states. In the AF_1 case, we constrain the total moment and find an energy minimum for $M=0$ with equal and opposite local moments of $1.6\mu_B$. In the AF_2 case, we constrain the local moments to be equal and opposite ($M=0$) and find an energy minimum for local moments equal to $1.6\mu_B$. Thus the AF_1 and AF_2 calculations may be viewed as two different strategies for obtaining the same information. In both cases, we find an energy minimum for an antiferromagnetic state with local moments of $1.6\mu_B$. Finally, note that the AF_2 curve crosses the curve for the ferromagnetic constraint at $M\simeq 2.3\mu_B$. Thus, at $r_{WS}=2.68$ a.u., the interatomic exchange (J in the Heisenberg model) is antiferromagnetic for magnetic moments $\lesssim 2.3\mu_B$ and ferromagnetic for magnetic moments $\gtrsim 2.3\mu_B$.

Having shown that AF_1 and AF_2 yield the same basic information, we now discuss the AF_1 calculations for finite total moments. Operationally, we perform FSM calculations as a function of volume for a CuAu unit cell with two inequivalent atoms. As shown in Fig. 1, we first find the antiferromagnetic solution at $M=0$ given by the AF_1 curve. As a function of increasing moment, we follow this antiferromagnetic branch with field-induced inequivalent local moments, to approximately M

$=1.1\mu_B$/atom where it ends abruptly. At this point, an instability develops and the total energy drops to the branch corresponding to a ferromagnetic constraint which is characterized by equal (and parallel) local moments. Continuing to higher moments, the system exhibits first a low-spin, and finally a high-spin, solution. Starting at high moments we can "lock" into this ferromagnetic mode and, by decreasing M, can trace this branch back through the instability region near $1.1\mu_B$ to zero moment, where we find the nonmagnetic solution. As a check of our internal consistency, we note that this second branch is (almost) identical to the corresponding curve shown in Fig. 3 in Ref. 12. The present work demonstrates the existence of an antiferromagnetic solution with a lower energy than the ferromagnetic solution in the low-moment range.

Zero-field solutions obtained from local minima of curves like the AF_1 curve (with its extension to the ferromagnetic branch) of Fig. 1 yield the volume dependence of the local moments and total energies shown in Fig. 2 for iron, and shown in Fig. 3 for manganese. Note that, in addition to the NM, LS, and HS solutions reported in Ref. 12 for iron, we now find a solution, labeled AF, beginning at the equilibrium (zero-pressure) volume and extending up to large volumes. This AF solution extends up to the free-atom limit, where it joins asymptotically with the HS solution. We find similar behavior for manganese. The curious dip in the AF branch of the moment versus r_{WS} curve occurs at volumes near the LS state. In both cases, the onset of antiferromagnetic behavior is second order, occurs at equilibrium (zero pressure), and is singular (infinite dM/dV). For iron the AF solutions are lower in energy than other solutions from $r_{WS}=2.54$ a.u. (the equilibrium volume, where the AF and NM solutions are degenerate) up to $r_{WS}=2.71$ a.u. (the crossing point of the AF and HS solutions) in general agreement with the work of Wang *et al.*[8] Our calculations therefore show a second-order transition from NM to AF behavior at $r_{WS}\simeq 2.54$ a.u., and a first-order transition from AF to HS behavior at $r_{WS}\simeq 2.71$ a.u. For manganese, the antiferromagnetic solutions are lower in energy from the equilibrium volume up to the free-atom limit, implying a second-order transition from NM to AF at $r_{WS}\simeq 2.58$ a.u.

Since all local moments and effective magnetic fields are constrained to be collinear, our results for behavior in the presence of a field (e.g., the AF_1 curve of Fig. 1) implicitly assume infinite anisotropy. In practice, application of an external field to an antiferromagnetic system will result in noncollinear local moments. Thus we do not consider rotation of the local moments relative to each other or to the field direction. With this infinite anisotropy condition, an effective external field results in collinear but unequal local moments. Local moments corresponding to AF_1 calculations for fcc iron and manganese at selected r_{WS} values are shown in Figs. 4 and 5,

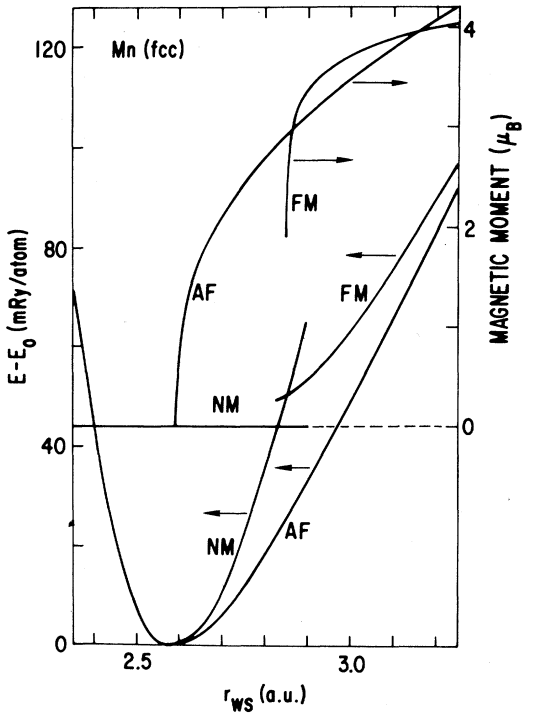

FIG. 3. Zero-field magnetic moments and total energies as a function of r_{WS} showing nonmagnetic, antiferromagnetic, and ferromagnetic solutions for fcc manganese.

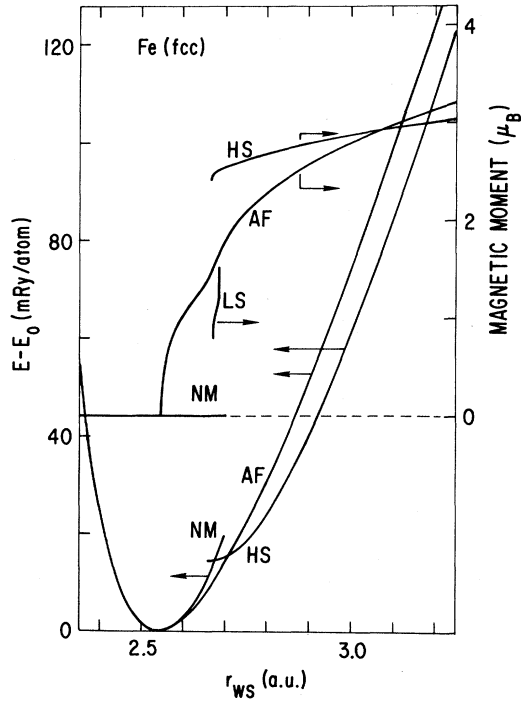

FIG. 2. Zero-field magnetic moments and total energies as a function of r_{WS} showing nonmagnetic (NM), antiferromagnetic (AF), low-spin (LS) and high-spin (HS) solutions for fcc iron. The LS total-energy branch is indistinguishable from the NM branch on this scale.

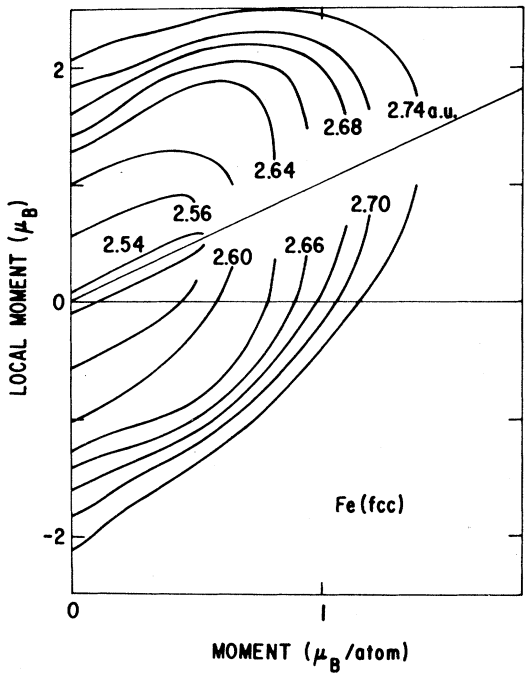

FIG. 4. Field-induced local moments for fcc iron in the infinite anisotropy limit as a function of fixed total moment for selected Wigner-Seitz radii. The diagonal line with a slope of unity corresponds to local moments for a ferromagnetic constraint (equal local moments).

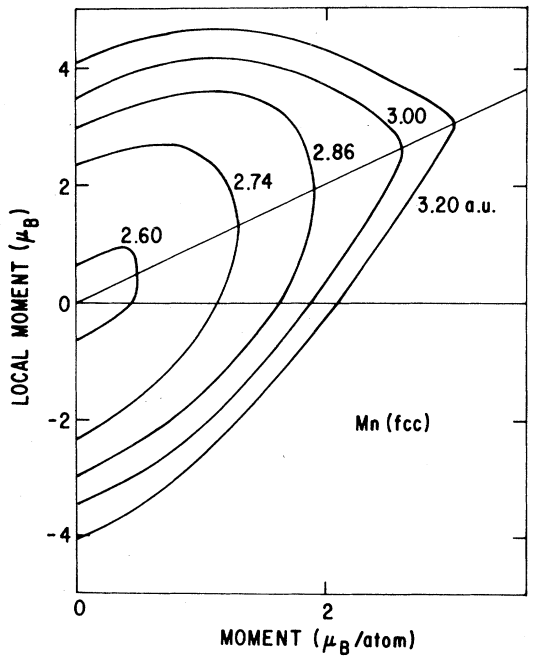

FIG. 5. Field-induced local moments for fcc manganese in the infinite anisotropy limit as a function of fixed total moment for selected Wigner-Seitz radii. The diagonal line with a slope of unity corresponds to local moments for a ferromagnetic constraint (equal local moments).

respectively. For a given volume, the magnitude of the up-spin local moment increases with increasing total moment. The magnitude of the down-spin local moment decreases to keep the sum equal to the fixed (imposed) total moment. The diagonal line corresponds to the ferromagnetic constraint with equal and parallel local moments. For iron, instabilities like that at $M=1.1\mu_B$ discussed above for $r_{WS}=2.68$ a.u. lead to a blank region where self-consistency is difficult to achieve. The curious curvature starting at $r_{WS}=2.64$ a.u. appears to be a consequence of the proximity of LS solutions apparent in Fig. 2. Manganese, which does not exhibit a LS state, also shows no sign of instabilities and has a more regular local moment behavior.

III. DISCUSSION

The results described in this work differ in detail from previous results.[6–9] We note that previous work did not specifically report the singular nature of the onset of antiferromagnetic behavior, nor the coincidence of the onset with the equilibrium zero-pressure points. In addition, we have extended the range to larger volumes, and have explored the ferrimagnetic behavior of fcc iron and manganese as the two-atom unit cell acquires a finite moment. The present calculations failed to reveal stable, zero-field ferrimagnetic solutions, but there are indications that such behavior is impending in fcc iron and may occur in other systems.

Bulk fcc iron calculations excluding antiferromagnetic behavior yield NM, LS, and HS solutions. With increasing volume, the system undergoes two successive first-order transitions (from NM to LS to HS). For manganese, we find a single first-order transition in the vicinity of $r_{WS}=2.85$ a.u. These first-order transitions correspond to magnetovolume instabilities. The antiferromagnetic solutions tend to remove these instabilities and allow both systems to develop magnetic properties more gently. For iron, the antiferromagnetic solution is preferred (has the lowest energy) throughout the narrow volume range of existence for the LS state. At $r_{WS}\simeq 2.71$ a.u. the system still undergoes a first-order transition from antiferromagnetic to ferromagnetic (HS) behavior. This transition represents a remaining magnetovolume instability that may change with the use of different constraints (e.g., other types of antiferromagnetic order or noncollinear local moments).

Our results for fcc iron differ from those of Wang *et al.*[8] in the position of the antiferromagnetic transition (we find the transition at a larger volume), in the initial form of the $M(V)$ curve (our curve rises with infinite slope at the transition), and in the range of existence for the LS state (we find a much more restricted range contained entirely within the high-spin regime). Our results for fcc manganese differ from those of Brener *et al.*[18] by displaying the antiferromagnetic solution along with total energies for both ferromagnetic and antiferromagnetic states.

Since the position of the transition from nonmagnetic to antiferromagnetic behavior for both fcc iron and manganese coincides with the equilibrium, or zero-pressure

Wigner-Seitz radii, the two solutions are degenerate at this volume. However, our results imply antiferromagnetic order with increasing local moments for systems which are epitaxially "clamped" at volumes larger than equilibrium. At volumes less than equilibrium, zero local moments are expected. We note that, as in the case of the onset of ferromagnetic order,[20] the onset of antiferromagnetic order is singular, i.e., dM/dV is infinite (here M is the sublattice magnetization). This is a direct consequence of the change in sign of the curvature of the energy versus moment curves at $M=0$ as a function of changing volume in going through the transition.

The curvature of the binding curve (total energy versus volume) at equilibrium is a direct measure of the bulk modulus. Since the systems studied here have second-order transitions from nonmagnetic to antiferromagnetic behavior coincident with the equilibrium volumes, the curvature at equilibrium is, in fact, discontinuous. Theoretical determination of the bulk modulus, therefore, depends upon whether the nonmagnetic or antiferromagnetic curvature is used. For fcc manganese, the curvature derived from the nonmagnetic branch, which extends both above and below the equilibrium volume, yields a bulk modulus of approximately 3000 kbar. The curvature for the antiferromagnetic branch, which only extends above the equilibrium volume, yields approximately 1100 kbar. This latter value is in good agreement with experiment.[21]

[1]P. Ehrhart, B. Schönfeld, H. H. Ettwig, and W. Pepperhoff, J. Magn. Magn. Mater. **22**, 79 (1980).
[2]W. A. A. Macedo and W. Keune, Phys. Rev. Lett. **61**, 475 (1988).
[3]M. Stampanoni, A. Vaterlaus, M. Aeschlimann, F. Meier, and D. Pescia (unpublished).
[4]E. F. Wassermann, Adv. Solid State Phys. **27**, 85 (1987).
[5]F. Jona (private communication).
[6]J. Kübler, Phys. Lett. **81A**, 81 (1981).
[7]J. Kübler (unpublished).
[8]C. S. Wang, B. M. Klein, and H. Krakauer, Phys. Rev. Lett. **54**, 1852 (1985).
[9]F. J. Pinski, J. Staunton, B. L. Gyorffy, D. D. Johnson, and G. M. Stocks, Phys. Rev. Lett. **56**, 2096 (1986).
[10]J. Kübler, J. Magn. Magn. Mater. **20**, 107 (1980).
[11]J. L. Fry, Y. Z. Zhao, P. C. Pattnaik, V. L. Moruzzi, and D. A. Papaconstantopoulos, J. Appl. Phys. **63**, 4060 (1988).
[12]V. L. Moruzzi, P. M. Marcus, K. Schwarz, and P. Mohn, Phys. Rev. B **34**, 1784 (1986).
[13]A. R. Williams, V. L. Moruzzi, J. Kübler, and K. Schwarz, Bull. Am. Phys. Soc. **29**, 278 (1984); K. Schwarz and P. Mohn, J. Phys. F **14**, 1129 (1984).
[14]G. L. Krasko, Phys. Rev. B **36**, 8565 (1987).
[15]P. M. Marcus and V. L. Moruzzi, Phys. Rev. B **38**, 6949 (1988).
[16]E. C. Stoner, Proc. R. Soc. London, Ser. A **169**, 339 (1939).
[17]V. L. Moruzzi, P. M. Marcus, and P. C. Pattnaik, Phys. Rev. B **37**, 8003 (1988); P. M. Marcus and V. L. Moruzzi, J. Appl. Phys. **83**, 4045 (1988); V. L. Moruzzi and P. M. Marcus, J. Appl. Phys. **64**, 5598 (1988).
[18]N. E. Brener, G. Fuster, J. Callaway, J. L. Fry, and Y. Z. Zhao, J. Appl. Phys. **63**, 4057 (1988).
[19]A. R. Williams, J. Kübler, and C. D. Gelatt, Jr., Phys. Rev. B **19**, 6094 (1979).
[20]V. L. Moruzzi, Phys. Rev. Lett. **57**, 2211 (1986).
[21]V. L. Moruzzi, A. R. Williams, and J. F. Janak, Phys. Rev. B **15**, 2845 (1977), and references therein.